

# CONSTRUCTION MECHANICS СТРОИТЕЛЬНАЯ МЕХАНИКА



UDC 624.44:539.376

Original Empirical Research

<https://doi.org/10.23947/2949-1835-2025-4-1-54-67>

## Examples of Testing a Program for Modeling Long-Term Deformation of Prestressed Reinforced Concrete Beams




EDN: KDXNZY

Peter P. Gaydzhurov<sup>1</sup>  , Elvira R. Iskhakova<sup>2</sup> , Nina A. Savelyeva<sup>1</sup> 

<sup>1</sup> Don State Technical University, Rostov-on-Don, Russian Federation

<sup>2</sup> South Russian State Polytechnic University (NPI) named after M.I. Platov, Novocherkassk, Russian Federation

 [gpp-161@yandex.ru](mailto:gpp-161@yandex.ru)

### Abstract

**Introduction.** Currently, there is very little information in the Russian literature on the development and practical application of numerical methods for studying the stress-strain state of concrete and reinforced concrete structures, taking into account the creep of concrete. As a rule, when analyzing the long-term deformation of such structures, calculators apply an empirical approach based on the use of the reduced modulus of deformation in combination with the coefficient of creep. The purpose of this study is to verify and validate the developed finite element algorithm and the corresponding software based on the results of experimental studies of the stress-strain state, prestressed reinforced concrete beam structures, taking into account the creep of concrete, available in the literature.

**Materials and Methods.** As a mathematical tool for modeling the process of long-term deformation of reinforced concrete girder structures, the finite element method was used in combination with a simple procedure for numerical integration along the time coordinate of the operator-matrix resulting equation. The program code is implemented on the basis of the Microsoft Visual Studio computing platform and the Intel Parallel Studio XE compiler with the built-in Intel Visual Fortran Composer XE text editor. The processes of storing and processing working arrays are implemented in terms of sparse matrices. The descriptive graphics of the Matlab computer system were used to visualize the calculation results. All of the computational experiments were performed using the authorized Polygon complex. The objectives of the study include evaluating the accuracy of the proposed methodology for analyzing the long-term deformation of reinforced concrete structures with various methods of external force action, including the effect of prestressing.

**Results.** A program for calculating reinforced concrete beam structures in a three-dimensional formulation has been developed and debugged using a discrete reinforcement scheme, according to which the reinforcing frame is modeled by rod (beam), and the concrete array by volumetric finite elements. To determine the restoring force caused by the tension of the cable reinforcement on concrete, a two-dimensional finite element model consisting of truss and spring finite elements is used. The simulation of long-term deformation was performed within the framework of the theory of linear viscoelasticity in combination with the principle of superposition of influences.

**Discussion and Conclusion.** A comparative analysis of the results of field and computational experiments on the stress-strain state of reinforced concrete beams of rectangular cross-section with post- and prestress is performed. The proposed method makes it possible to calculate prestressed reinforced concrete girder structures with variable quasi-static loading, taking into account the linear creep of concrete.

**Keywords:** finite element method, creep of concrete, pre-tensile stress, reinforced concrete girder structures

**For citation.** Gaydzhurov PP, Iskhakova ER, Savelyeva NA. Examples of Testing a Program for Modeling Long-Term Deformation of Prestressed Reinforced Concrete Beams. *Modern Trends in Construction, Urban Planning and Territorial Planning*. 2025;4(1):54–67. <https://doi.org/10.23947/2949-1835-2025-4-1-54-67>

## Примеры тестирования программы моделирования длительного деформирования предварительно напряженных железобетонных балок

П.П. Гайджуrow<sup>1</sup> , Э.Р. Исхакова<sup>2</sup> , Н.А. Савельева<sup>1</sup> 

<sup>1</sup> Донской государственный технический университет, г. Ростов-на-Дону, Российская Федерация

<sup>2</sup> Южно-Российский государственный политехнический университет (НПИ) имени М.И. Платова,

г. Новочеркасск, Российская Федерация

✉ [gpp-161@yandex.ru](mailto:gpp-161@yandex.ru)

### Аннотация

**Введение.** В настоящее время в отечественной литературе приведено крайне мало сведений о разработке и применении на практике численных методов исследования напряженно-деформированного состояния бетонных и железобетонных конструкций с учетом ползучести бетона. Как правило, при анализе длительного деформирования подобных конструкций расчетчики применяют эмпирический подход, основанный на использовании коэффициента ползучести. Цель настоящего исследования заключается в верификации и валидации разработанного конечно-элементного алгоритма и соответствующего программного обеспечения на базе имеющихся в литературе результатов экспериментальных исследований напряженно-деформированного состояния предварительно напряженных железобетонных балочных конструкций с учетом ползучести бетона.

**Материалы и методы.** В качестве математического аппарата для моделирования процесса длительного деформирования железобетонных балочных конструкций применен метод конечных элементов в сочетании с шаговой процедурой численного интегрирования по временной координате результирующего операторно-матричного уравнения. Программный код реализован на базе вычислительной платформы Microsoft Visual Studio и компилятора Intel Parallel Studio XE со встроенным текстовым редактором Intel Visual Fortran Composer XE. Процессы хранения и обработки рабочих массивов реализованы в терминах разреженных матриц. Для визуализации результатов расчетов использована дескрипторная графика компьютерной системы Matlab. Все вычислительные эксперименты выполнены с помощью авторизованного комплекса Polygon. В задачи исследования входит оценка точности предлагаемой методики анализа длительного деформирования железобетонных конструкций при различных способах внешнего силового воздействия, включая эффект предварительного напряжения.

**Результаты исследования.** Разработана и отлажена программа расчета железобетонных балочных конструкций в трехмерной постановке с использованием дискретной схемы армирования, согласно которой армирующий каркас моделируется стержневыми (балочными) конечными элементами, а массив бетона — объемными. Для определения восстанавливающего усилия, обусловленного натяжением тросовой арматуры на бетон, применена двухмерная конечно-элементная модель, состоящая из ферменных и пружинных конечных элементов. Моделирование длительного деформирования выполнено в рамках теории линейной вязкоупругости в сочетании с принципом наложения воздействий.

**Обсуждение и заключение.** Выполнен сравнительный анализ результатов натуральных и вычислительных экспериментов исследования напряженно-деформированного состояния железобетонных балок прямоугольного поперечного сечения с пост- и преднапряжением. Предлагаемая методика позволяет выполнить расчет предварительно напряженных железобетонных балочных конструкций при переменном характере квазистатического нагружения с учетом линейной ползучести бетона.

**Ключевые слова:** метод конечных элементов, ползучесть бетона, предварительное напряжение, железобетонные балочные конструкции

**Для цитирования.** Гайджуrow П.П., Исхакова Э.Р., Савельева Н.А. Примеры тестирования программы моделирования длительного деформирования предварительно напряженных железобетонных балок. *Современные тенденции в строительстве, градостроительстве и планировке территорий*. 2025;4(1):54–67. <https://doi.org/10.23947/2949-1835-2025-4-1-54-67>

**Introduction.** It is widely known that concrete has been the most common building material over the last two centuries. There have been hundreds of unique high-rise buildings all over the world constructed using high-strength concrete structurally reinforced with a steel frame, offshore platforms for hydrocarbon production as well as protective shells of nuclear reactors have also been manufactured. It is difficult to imagine hydropower, large-span bridges, subways, large-scale motorway interchanges and transport tunnels without concrete. However, unlike steel, which is no less common in construction, concrete is much more susceptible to creep deformation that largely depends on the "age" of the binder, the

size of the structure, the nature and sequence of application or removal of external loads, as well as the temperature and humidity conditions of the environment. It has been experimentally found that creep has a considerable impact on the redistribution of internal forces in concrete and reinforced concrete structures. Moreover, the displacements caused by creep deformation can be several times higher than those caused by the application of the load at the initial moment of time. There is now a significant amount of experimental and theoretical material available on concrete creep. At the same time, the well-known approaches to calculating concrete and reinforced concrete structures taking into account creep are mostly focused on solving problems with a relatively simple product geometry and they fail to take into account the technological background associated with the formation of the initial stress state and the effect of inheritance of the stress-strain due to the history of loading the structure. Therefore, we are being faced with a pressing problem of developing a more general finite element algorithm implementing a model of an elastic creeping body allowing one to consider the effect of rapidly increasing creep at the time of application of an operational load, the partial reversibility of creep deformation while removing a long-acting load (elastic after-impact), various methods and schemes of reinforcement prestressing.

The objective of the study is to test an authorized finite element software package by means of comparing the results obtained with other authors' data.

**Materials and Methods.** In compliance with G.N. Maslov — N.H. Harutyunyan's assumption, the total relative longitudinal deformation  $\delta(t, \tau)$  of a prismatic concrete sample during compression is commonly represented as the following sum [1–4]:

$$\delta(t, \tau) = \frac{1}{E(t)} + C(t, \tau),$$

where  $\tau$  is the parameter corresponding to the "age" of the concrete;  $\frac{1}{E(t)}$  is the elastic instantaneous deformation of the sample;  $E(t)$  is the the current value of the modulus of deformation;  $C(t, \tau)$  is the creep deformation at the time of observation  $t$  ( $\tau \leq t < \infty$ ).

The function  $C(t, \tau)$  is commonly referred to as the creep measure. Depending on the type of the function  $C(t, \tau)$ , creep deformation following unloading can be completely or partially reversible [5]. As noted in [1, 3, 4], it is convenient to approximate the function  $E(t)$  using the following dependence:

$$E(t) = E_0(1 - \xi e^{-\beta t}),$$

where  $E_0$  is the limiting value of the modulus of elasticity of "mature age" concrete.

The parameters  $\xi, \beta$  included in the expression  $E(t)$  are determined experimentally and depend on the composition and conditions of concrete hardening.

These are the expressions for the creep measure function:

by N.H. Harutyunyan [1]:

$$C(t, \tau) = \varphi(\tau)[1 - e^{-\gamma(t-\tau)}]; \tag{1}$$

by S.V. Aleksandrovskiy [3]:

$$C(t, \tau) = \psi(\tau) - \psi(t) \left( \frac{1 - A_2 e^{-\gamma\tau}}{1 - A_2 e^{-\gamma t}} \right) e^{-\gamma(t-\tau)} + \Delta(\tau)[1 - e^{-\alpha(t-\tau)}]. \tag{2}$$

The rapidly decreasing functions here are the following:

$$\varphi(\tau) = C_1 + \frac{A_1}{\tau}, \psi(\tau) = C_3 + \frac{A_3}{\tau}, \Delta(\tau) = C_1 - C_3 + \frac{A_1 - A_3}{\tau}.$$

It should be noted that the function  $\varphi(\tau)$  was first set forth by N.H. Harutyunyan [1]. The graph of the function  $\varphi(\tau)$  for various parameter values  $C_1$  and  $A_1$  is shown in Fig. 1. In this figure, the curves  $\varphi(\tau)$  tend to the limiting value  $C_1/A_1$ . The constants in expressions (1) and (2) in units of measurement adopted in [3] are

$$\alpha = 6 \text{ day}^{-1}; \gamma = 0.03 \text{ day}^{-1}; A_1 = 4.62 \cdot 10^{-5} \frac{\text{day}}{\text{kgsec/cm}^2} (4.7095 \cdot 10^{-10} \frac{\text{day}}{\text{N/m}^2});$$

$$A_2 = 1; A_3 = 3.416 \cdot 10^{-5} \frac{\text{day}}{\text{kgsec/cm}^2} (3.48226 \cdot 10^{-10} \frac{\text{day}}{\text{N/m}^2}); C_1 = 0.975 \cdot 10^{-5} \text{ cm}^2/\text{kgsec} (9.9388 \cdot 10^{-10} \text{ m}^2/\text{N});$$

$$C_3 = 0.756 \cdot 10^{-5.5} \text{ cm}^2/\text{kgsec} (7.7064 \cdot 10^{-11} \text{ m}^2/\text{N}).$$

The values of the constants converted into the SI system are shown in the parentheses. The graph of the function  $C(t, \tau)$  for various values in the range  $t$  from 0 to 100 days while using the values of the constants in the SI system is shown in Fig. 2.

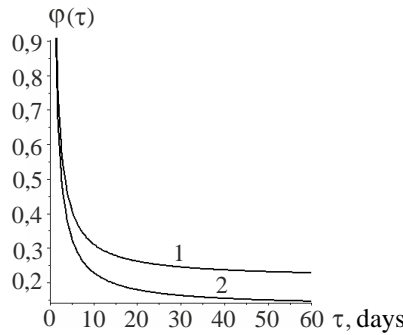


Fig. 1. Graph  $\varphi(\tau) = \frac{1}{A_1} \left( C_1 + \frac{1}{\tau} \right)$ :  
 1 —  $C_1 = 0.975 \cdot 10^{-5} \text{ cm}^2/\text{kgsec}$ ;  $A_1 = 4.62 \cdot 10^{-5} \text{ days} \cdot (\text{kgsec}/\text{cm}^2)^{-1}$ ;  
 2 —  $C_1 = 0.238 \cdot 10^{-5} \text{ cm}^2/\text{kgsec}$ ;  $A_1 = 1.85 \cdot 10^{-5} \text{ days} \cdot (\text{kgsec}/\text{cm}^2)^{-1}$

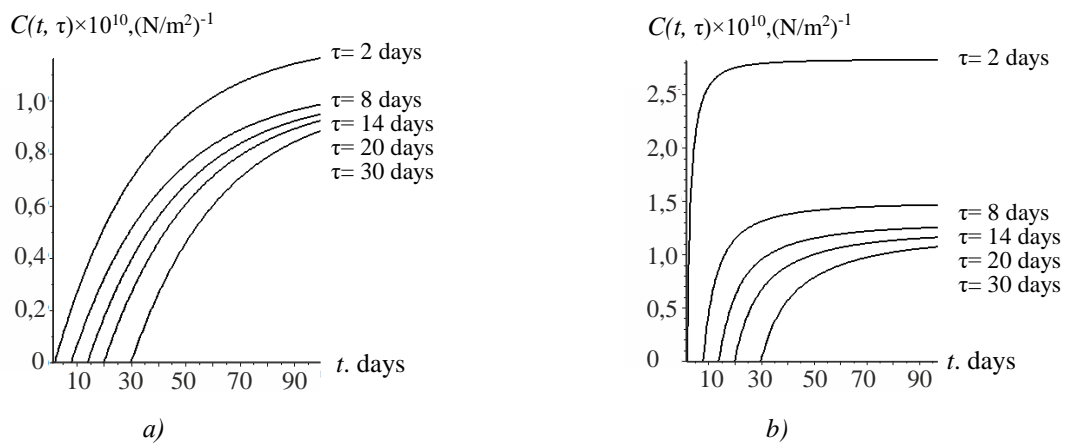


Fig. 2. Graphs of the functions  $C(t, \tau)$ :  $(\text{N}/\text{m}^2)^{-1}$   
 a – by N.H. Harutunyan [1]; b – by S.V. Aleksandrovskiy [3]

Comparing the graphs in Fig. 2, a and 2, b at  $\tau = 2$  days and  $t = 100$  days, we find that the values calculated using formula (2) are almost 2.5 times higher than the data based on formula (1). At  $\tau$  equalling 8, 14, 20, 30 days and  $t = 100$  days of the value of  $C(t, \tau)$  calculated using formulas (1) and (2) are not much different. It should also be noted that the initial steepness of the curves  $C(t, \tau)$  in Fig. 2, b is sharper than in Fig. 2, a.

For the finite element analysis of monolithic reinforced concrete structures taking into account the creep of concrete, the relationship between stresses and deformations is presented in the matrix operator form:

$$\{\sigma(t)\} = [E(t)](1 - R)\{\varepsilon(t)\},$$

where  $\{\sigma(t)\}$ ,  $\{\varepsilon(t)\}$  are the vectors-columns of the stresses and deformations corresponding to the moment of time  $t$ ;  $[E(t)]$  is the elasticity matrix (with the dimensionality  $6 \times 66 \times 66$  in the general case);  $R\varepsilon_{ij} = \int_{\tau_1}^t R(t, \tau)\varepsilon_{ij}(\tau)d\tau$ ,  $i, j = 1, 3$  is the linear integral operator establishing a correspondence between the current deformations  $\varepsilon_{ij}$  and the "history" of long-term deformation  $\varepsilon_{ij}(\tau)$ .

The so-called hereditary function  $R(t, \tau)$  is introduced in the expression under the integral sign. The type of hereditary function is known to determine how real modeling of a creep process is, particularly taking into account the system response when the load is partially or completely removed. In relation to the theory of creep of hereditary concrete, three major directions are identified [3, 4]: the theory of elastic heredity; the theory of aging; the theory of elastic-creeping body. Let us take a closer look at the main features of hereditary functions that are at the core of each of the above theories.

In the theory of elastic heredity, it is assumed that complete reversibility (zeroing) of deformations occurs during unloading. The hereditary function in this case takes the form [3]:

$$R(t - \tau) = E_0 C_1 \gamma e^{-\gamma(1 + E_0 C_1)(t - \tau)}, \tag{3}$$

where  $E_0$  is the initial elasticity modulus;  $C_1, \gamma$  are the constants identified experimentally using the creep curves.

The graph  $R(t, \tau)$  based on expression (3) for various values of the parameter  $\tau$  is shown in Fig. 3. Hereafter, the constants included in (3) are assumed to be the same as in expressions (1) and (2). The value of the initial modulus of elasticity of concrete  $E_0 = 2.55 \cdot 10^{10} \text{ N/m}^2$ . The computer mathematics environment of the Maple system was used to design the graph [6].

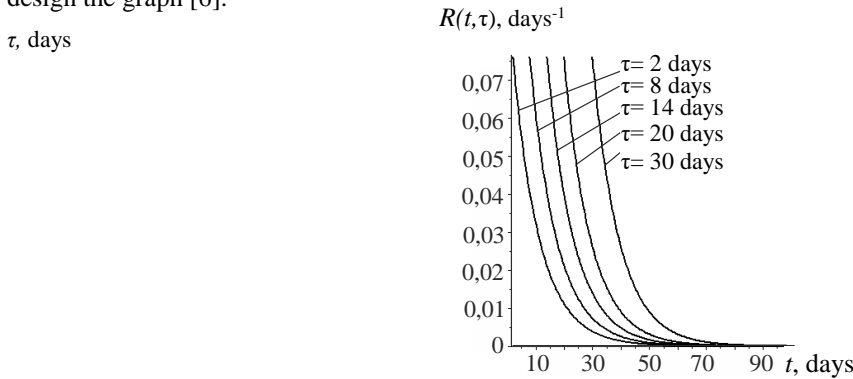


Fig. 3. Graph  $R(t, \tau)$  according to the theory of elastic heredity

As can be seen, the curves in Fig. 3 for various values of  $\tau$  mimic one another with a displacement. This is due to the fact that in expression (3) the modulus of elasticity is assumed to be constant, i.e. the effect of "aging" of the material is not considered in this theory. The theory of elastic heredity is only applicable to "old" concrete. In this case, it is assumed that the creep deformation depends only on the duration of the operating load.

The theory of aging relies on the assumption that the reversibility of creep deformations during partial or complete unloading is completely denied. The expression for the function  $R(t, \tau)$  taking into account the change in the deformation properties of the material over time provided in the biography of S.V. Alexandrovsky [3] takes the following form:

$$R(t, \tau) = \frac{1}{E(t)} \cdot \frac{\partial}{\partial \tau} \left[ E(\tau) e^{-\int_{\tau}^t E(\tau) \frac{\partial}{\partial \tau} C(\tau, \tau_1) d\tau} \right], \quad (4)$$

where  $E(t) = E_0(1 - e^{-\beta t})$  is an approximation of the modulus of elastic deformations (parameter =  $0.206 \text{ days}^{-1}$ );  $\tau_1$  is "age" of concrete at the time of loading, days.

Visualization of the function  $R(t, \tau)$  in the form of a graph based on expression (4) in the Maple environment is shown in Fig. 4.

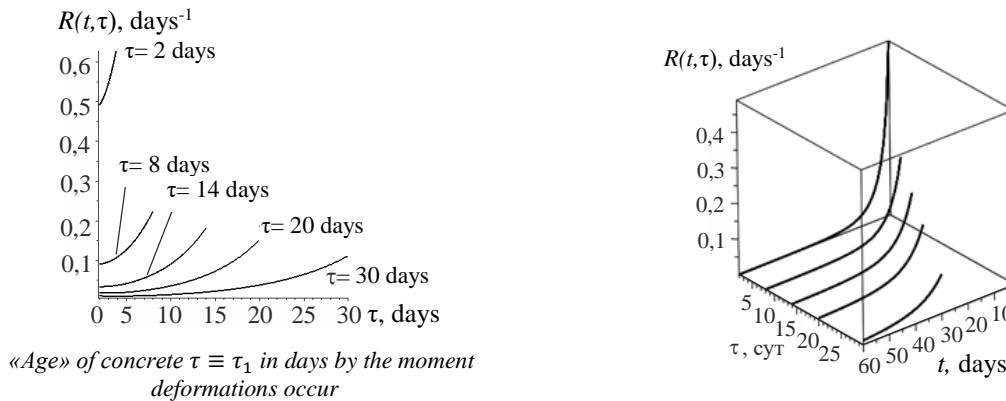


Fig. 4. Graph  $R(t, \tau)$  according to the theory of aging

As noted in [3], the theory of aging is applicable for calculations of concrete and reinforced concrete structures under a short-term load. Furthermore, in the case of unloading, this theory causes a considerable overestimation of the aftereffect deformations for "young" concrete and an underestimation of those for "old" concrete.

The theory of elastic-creeping body takes into consideration the partial reversibility of creep deformations during unloading. In the monograph by S.V. Aleksandrovsky [3] within the framework of the theory of elastic-creeping body the following expression for the hereditary function of concrete is set forth:

$$R(t, \tau) \approx -\frac{1}{E(t)} K^2(\tau) F'(\tau) (e^{\gamma\tau} - A_2) - K'(\tau) - [K(\tau)(e^{\gamma\tau} - A_2)e^{-\eta(\tau)}] \int_{\tau}^t K(\tau) F'(\tau) e^{\eta(\tau)} d\tau + B_3(t) e^{-\mu(t)(t-\tau)}, \quad (5)$$

where  $(\dots)' = \partial \dots / \partial \tau$ ;  $B_3(t) = F'(t)(e^{\gamma t} - A_2)[E^2(t) - K^2(t)] - \alpha E^2(t)\Delta(t) + K'(t) - E'(t)$ ;

$$\begin{aligned} \mu(t) = & \frac{1}{B_3(t)} \{ B_3'(t) + \gamma e^{\gamma t} F'(t) [E^2(t) - K^2(t)] - \\ & - F'^2(t) (e^{\gamma t} - A_2)^2 [E^3(t) - K^3(t)] - \alpha E(t) [E(t)\Delta(t)]' - \\ & - \alpha^2 E^3(t) \frac{\Delta(t)}{K(t)} + \frac{1}{2} F'(t) (e^{\gamma t} - A_2) [E^2(t) - K^2(t)]' + \\ & + 2\alpha E^3(t) \Delta(t) F'(t) (e^{\gamma t} - A_2) \}; \\ K(t) = & \frac{E(t)}{1 + \Delta(t)E(t)}. \end{aligned}$$

For a rapidly decreasing function  $\Delta(t)$ , the following dependencies are set forth in the monograph [3]:

- 1)  $\Delta(t) = (0.25 + 0.99^{-at}) \cdot 10^{-5}$ ;
- 2)  $\Delta(t) = C_1 - C_3 + \frac{A_1 - A_3}{t}$ ;
- 3)  $\Delta(t) = \left(\frac{80}{t} + 2.714\right) \cdot 10^{-7}$ ;
- 4)  $\Delta(t) = (11.2 + 34 \cdot e^{-0.125 \cdot t}) \cdot 10^{-7}$ .

The graph of the function  $\Delta(t)$  designed using the above expressions for  $\Delta(t)$  is shown in Fig. 5. The numbers indicate the curves corresponding to the dependency numbers  $\Delta(t)$ .

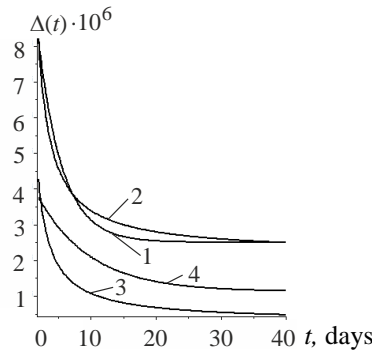


Fig. 5. Graph of the function  $\Delta(t)$  for dependencies 1, 2, 3, 4

Given the qualitative coincidence of the curves  $\Delta(t)$  in Fig. 5, in the future a more universal dependence (2) will be used.

In order to make formula (5) look convenient for programming, the symbolic processor of the Maple system [6] will be used. The curves of the function  $R(t, \tau)$  for different "ages" of concrete obtained by means of computational technology [7] are shown in Fig. 6. Figure 7 shows a similar graph  $R(t, \tau)$  from the monograph [3]. The range of variation of the parameter in Fig. 6 and 7 is almost identical.

Comparing the graphs  $R(t, \tau)$  in Fig. 6 and 7, it is found that that the curves of the hereditary function are identical within the visualization for the same parameter values. It is critical to note that the curves  $R(t, \tau)$  shown in Fig. 6 are clearly indicative of the consideration of the so-called rapidly increasing creep observed in practice at a moment in time  $t = \tau + \delta t$  where  $\delta t \leq 1$  day [3].

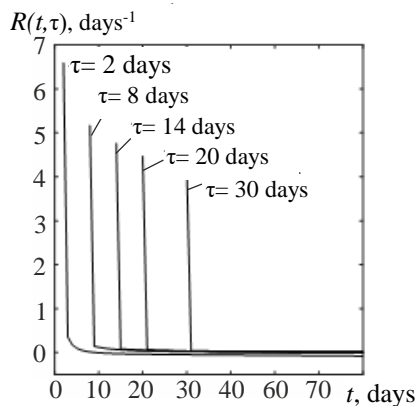


Fig. 6. Graph  $R(t, \tau)$  [7]

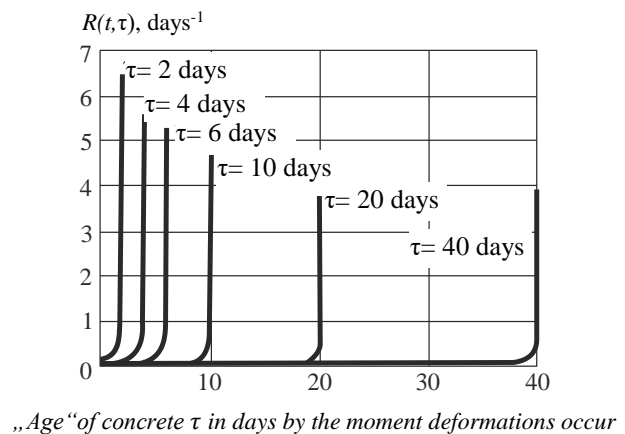


Fig. 7. Graph  $R(t, \tau)$  [3]

For "old" concrete, the following expression for the hereditary function is recommended in the monograph [3]:

$$R(t - \tau) = A_1 e^{-\rho_1(t-\tau)} + A_2 e^{-\rho_2(t-\tau)}, \tag{6}$$

where

$$A_1 = \frac{E_0}{\rho_1 - \rho_2} \{(\gamma\psi_0 + \alpha\Delta_0)[E_0(\gamma\psi_0 + \alpha\Delta_0) - \rho_2] + \alpha^2\Delta_0 + \gamma^2\psi_0\};$$

$$A_2 = E_0(\gamma\psi_0 + \alpha\Delta_0) - A_1;$$

$$\rho_{1,2} = \frac{1}{2} \{ \alpha + \gamma + E_0(\gamma\psi_0 + \alpha\Delta_0) \pm \sqrt{E_0^2(\gamma\psi_0 + \alpha\Delta_0)^2 + (\alpha - \gamma)^2 - 2E_0(\gamma\psi_0 - \alpha\Delta_0)(\alpha - \gamma)} \}.$$

When calculating  $R(t - \tau)$  in expression (6), we assume  $\Delta(t) = \Delta_0 = const, \psi(t) = \psi_0 = const$ .

**Research Results.** As the first test example, let us look into the problem of prolonged deformation of a cylindrical prismatic concrete sample while compressed axially. The results of similar physical experiments are provided in [8]. The diameter and height of the prismatic sample as in [8] were assumed to be 12 cm and 30 cm, respectively. A pressure of 15 MPa was applied to the free end of the sample. Taking into consideration the axial symmetry of geometry and loading during finite element modeling, 1/4 of the prismatic sample was considered. The grid step was assumed to be uniform and equal to 1 cm. While boundary conditions were set, connections were introduced at the ends of the prism in order to prevent radial movements. Therefore the nodes of the free end have only one degree of freedom in the form of axial displacement.

For calculations the authorized Polygon complex [9, 10] is used. The obtained graphs  $u_z \sim t$  for two concrete models and two loading schemes are shown in Fig. 8. The initial modulus of elasticity of concrete is  $E = 2.8 \cdot 10^4$  MPa. The observation time is 200 days. The right-hand side of Fig. 8 shows a graph  $u_z \sim t$  for the loading and full unloading mode at  $t = 60$  days.

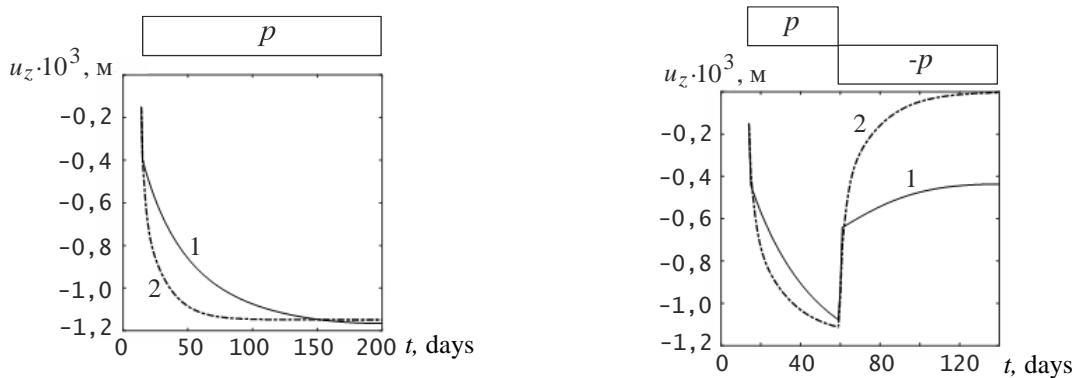


Fig. 8. Graphs of the movement of the prismatic sample: 1 — model of an elastic-creeping body (5); 2 — model of "old" concrete (6)

As can be seen, for the "old" concrete model (6), complete reversibility of creep deformation occurs during unloading.

Visualization of the distribution of axial displacement fields and stress intensity for the elastic-creeping body model (5) and time = 60 days is shown in Fig. 9 and 10.



Fig. 9. Distribution pattern in 1/4 of the prismatic sample at  $t = 60$  days

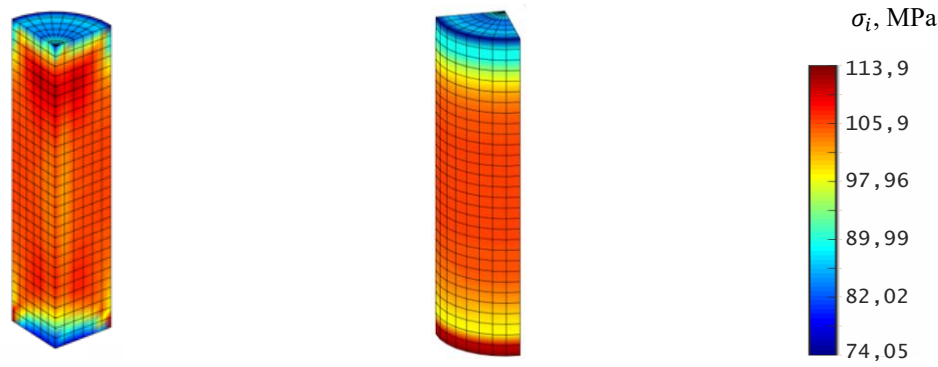


Fig. 10. Distribution pattern  $\sigma_i$  in 1/4 of the prismatic sample at  $t = 60$  days

Fig. 10 is clearly indicative of the impact of the accepted boundary conditions on the stress distribution over the height of the prism. The highest concentration  $\sigma_i = 113.9$  MPa is observed at the lower end of the sample.

In order to study the accuracy of the developed mathematical and software, the results of field experiments on the long-term creep of double-support beams under two-point loading provided in [11] were used. In these experiments, prestressed reinforced concrete beams were subjected to prolonged (over 4.5 years) force exposure. The constant load  $F = \text{const}$  was maintained by hydraulic jacks.

The loading scheme and cross-section options of the beams are shown in Fig. 11 and 12, respectively (the dimensions are in millimeters).

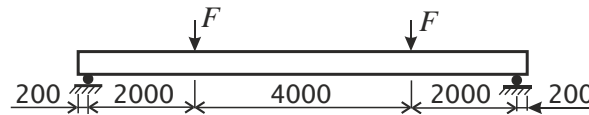


Fig. 11. Loading scheme of the beam

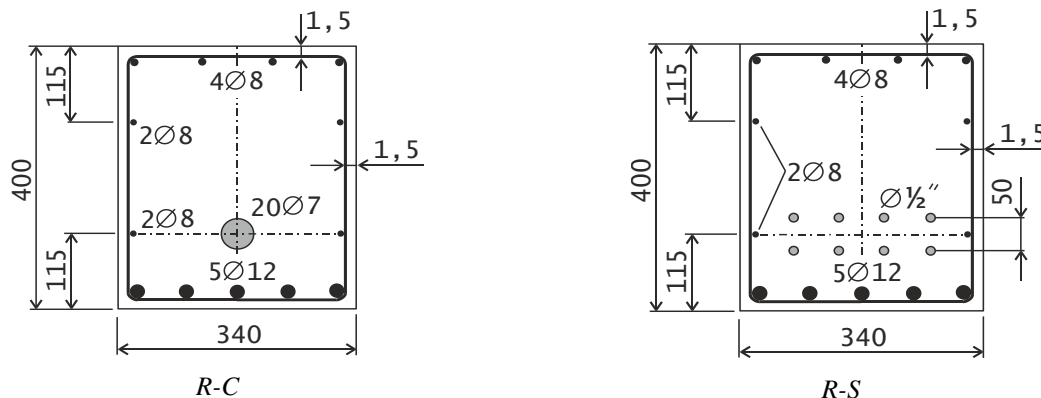


Fig. 12. Cross sections of RC and R-S series beams in the middle of the span [11]

These figures show the placement schemes of the "background" longitudinal and "active" prestressed fittings. According to the data [11], the initial stress state was generated in the beams of the R-C series by compressing concrete at the "age" of 28 days along the ends with cable reinforcement. These are the so-called post-stress beams. The cable was made up of twenty strands with a nominal diameter of 7.2 mm (the cross-sectional area of one strand was  $38.70 \text{ mm}^2$ ). The diagram of the trajectory of the "active" reinforcement of the R-C series beam is shown in Fig. 13. During testing, a beam variant with the following parameters was considered:  $a = 0.115 \text{ m}$ ;  $b = 0.227 \text{ m}$ . The tensile strength for a single strand is 1770 MPa.

The prestressing in the R-S series beam was created according to the scheme of tension of the reinforcement on the stops. 28 days after the concrete had been laid in the appropriate form, the "active" reinforcement had been "removed" from the stops, and the initial stress state occurred in the beam. The voltage in the "active" reinforcement for the R-C and R-S series beams was assigned based on the following condition:

$$\sigma = 0.7 f_{ptk}$$

Then for the R-C series beam we have:

$$F_{pr} = \sigma n A_{R-C} = 0.7 \cdot 1770 \cdot 10^6 \cdot 20 \cdot 38.7 \cdot 10^{-6} = 959 \text{ kN},$$

where  $n$  is the number of cable strands ( $n = 20$ );  $A_{R-C}$  is the cross-sectional area of the cable strand.



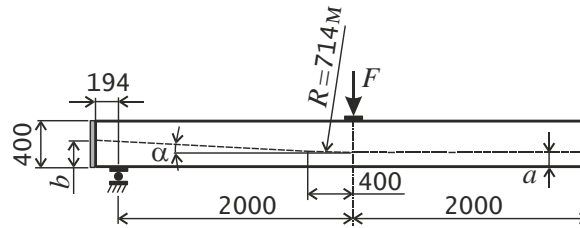


Fig. 13. Diagram of the trajectory of the "active" reinforcement of the 1/2 part of the R-C series beam

For a qualitative and quantitative assessment of the restoring effect caused by the tension of the rope in the beam of the R-C series, we use an auxiliary two-dimensional finite element model. This model is formed from truss and spring finite elements (Fig. 14). In this case, the vertical reactions in the spring elements  $r_i$  are equivalent to discrete values of the restoring forces.

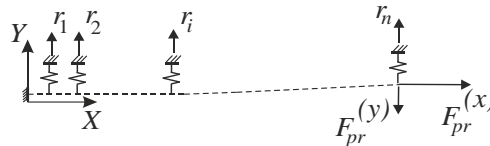


Fig. 14. Diagram for identifying the restoring force

As a result of the modelling, we get:  $F_{pr}^{(x)} = 958 \text{ kN}$ ;  $F_{pr}^{(y)} = 51.1 \text{ kN}$ . A plot of the distribution of the restorative efforts of Frest is shown in Fig. 15.

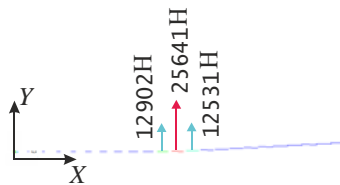


Fig. 15. A timeline of restorative efforts  $F_{rest}$

The prestress in the R-S series beam is created by eight cables  $\varnothing 1/2'$ . The nominal diameter of each cable is 10.9 mm (cross-sectional area  $93.3 \text{ mm}^2$ ). For this series, the tension force is given by the formula:

$$F_{pr} = 0.7 \cdot 1860 \cdot 10^{-6} \cdot 93.3 \cdot 10^{-6} = 121.4 \text{ kN}.$$

We assume that the effort  $q_{np}$  from the prestretched cable in the R-S series beam acts on a section with a length of  $l_p = 15 \cdot d$  where  $d$  is the diameter of the reinforcement (Fig. 16). The value  $q_{np}$  is defined as the ratio  $F_{pr}/l_p$ .

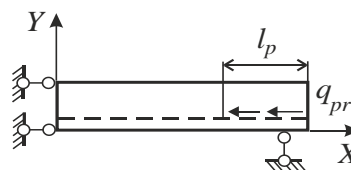


Fig. 16. Prestressing scheme in the R-S series beam

The design scheme for the 1/2 part of the R-C series beam and the corresponding finite element model with the allocation of an array of concrete and a reinforcing frame are shown in Fig. 17 and 18, respectively. The force applied to 1/2 part of the beam,  $F_{sust} = 63.75 \text{ kN}$ . In order to reduce the stress concentration in the force application zones and the support, pads with a thickness of 10 cm have been introduced. The material of the platforms is steel.

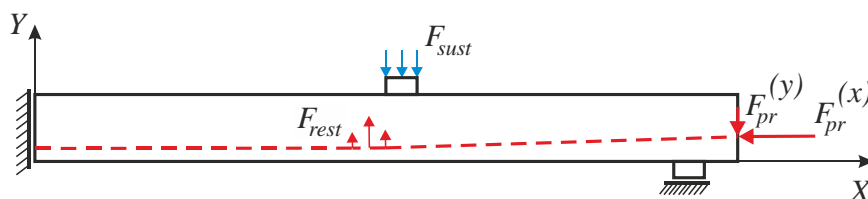


Fig. 17. Calculation scheme of 1/2 part of the R-C series beam

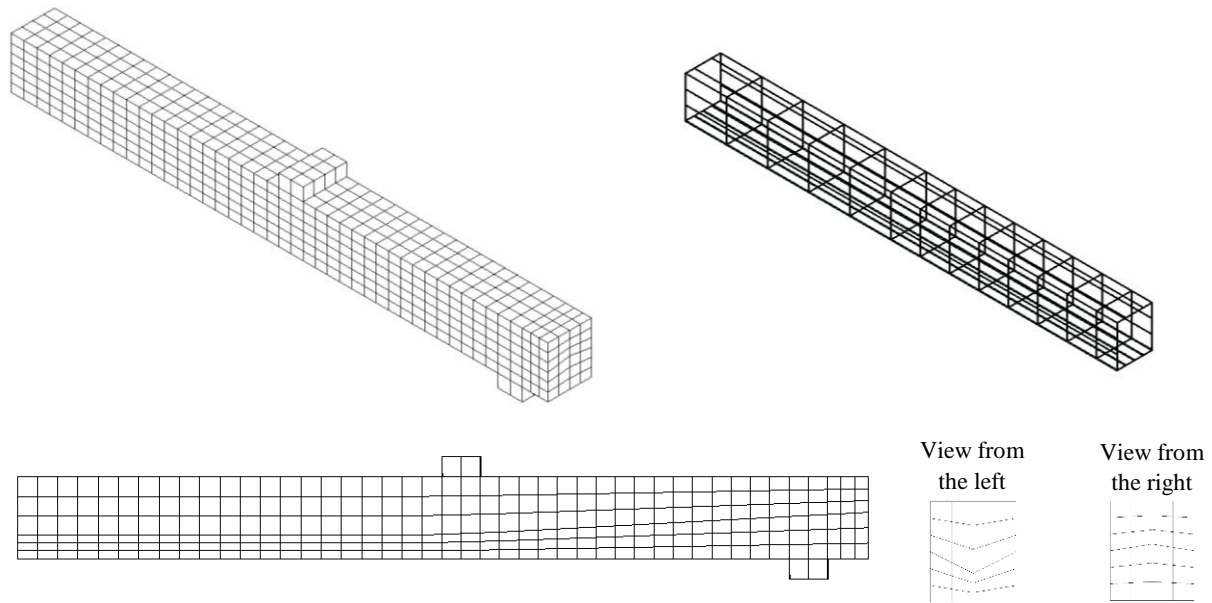


Fig. 18. Finite element model 1/2 part of the R-C series beam

The design scheme for the 1/2 part of the R-S series beam and the corresponding finite element model with the allocation of an array and a reinforcing frame are shown in Fig. 19 and 20, respectively.

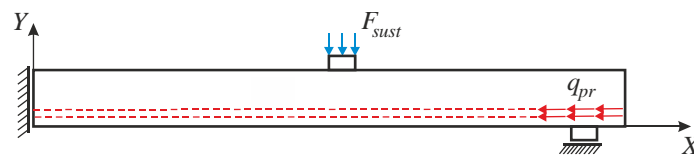


Fig. 19. Calculation scheme of 1/2 part of the R-S series beam

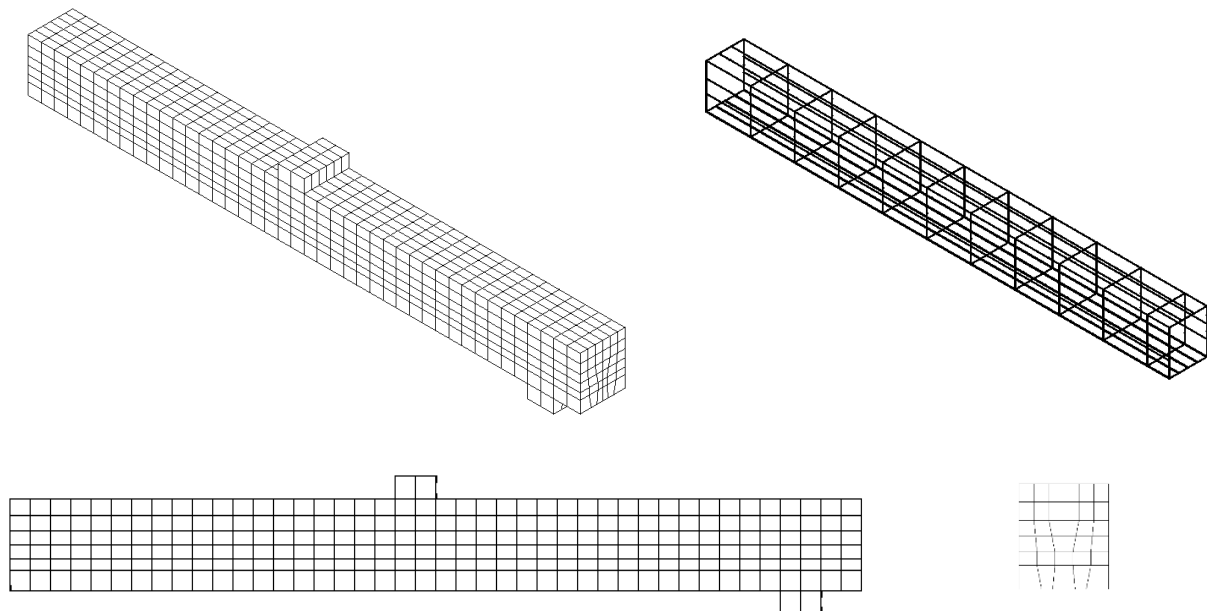


Fig. 20. Finite element model 1/2 part of the R-S series beam

The results of finite element modeling of deflection changes  $u_y$  in the center of the beam span of the R-C and R-S series at the stages of prestressing at the "age" of concrete for 14 days and loading with  $F_{sust}$  force at the time of 28 days are shown in Fig. 21, a. The estimated observation time was 100 days. Fig. 21, b shows the graphs  $u_y \sim t$  obtained experimentally [11].

As can be seen from Fig. 21, *a* and 21, *b*, the deflection values obtained numerically and experimentally at time points 28 days and 100 days almost coincide.

Visualization of longitudinal fields  $\sigma_{xx}$  and tangential  $\sigma_{xy}$  The stresses for the R-C series beam (time point 100 days) are shown in Fig. 22 and 23. Similar stress distribution patterns  $\sigma_{xx}$  and  $\sigma_{xy}$  The R-S series beams are shown in Fig. 24 and 25. Fig. 22-25 shows the beam fragments corresponding to the section  $0 \leq x \leq 3,71\text{m}$ , i.e., without a support area.

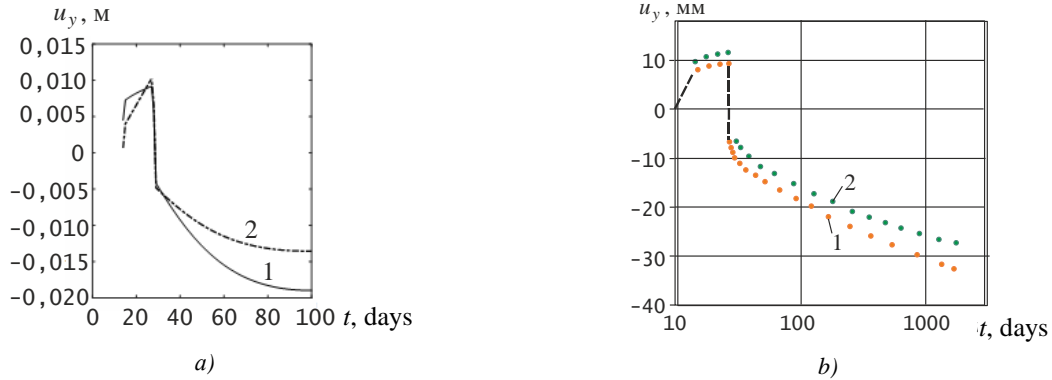


Fig. 21. Graphs  $u_y \sim t$ : 1 — R-C series beam; 2 — R-S series beam

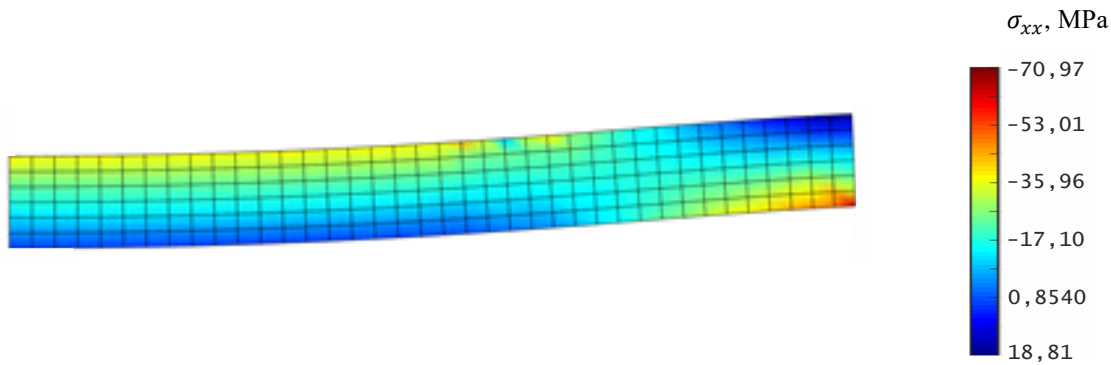


Fig. 22. Visualization of the distribution  $\sigma_{xx}$  for the R-C series beam,  $t = 100$  days

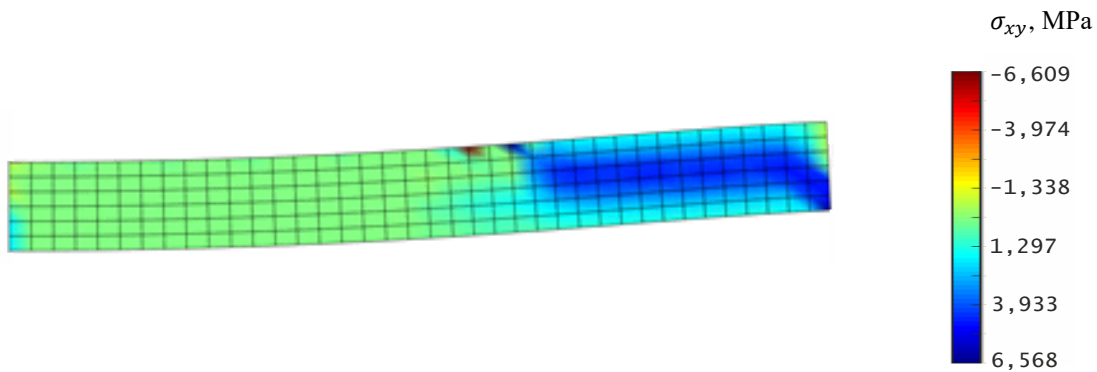


Fig. 23. Visualization of the distribution  $\sigma_{xy}$  for the R-C series beam,  $t = 100$  days

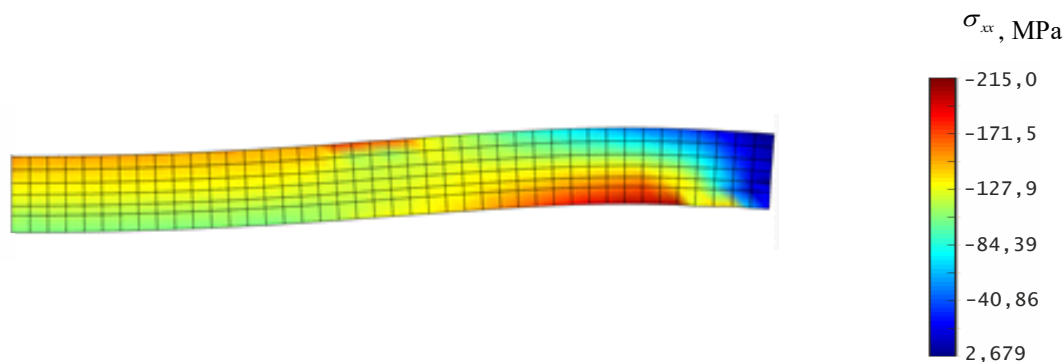


Fig. 24. Visualization of the distribution  $\sigma_{xx}$  for the R-C series beam,  $t = 100$  days

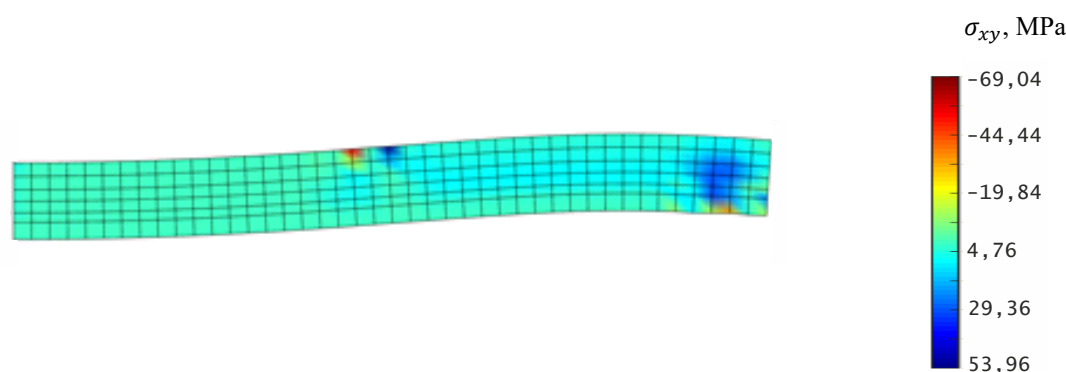


Fig. 25. Visualization of the distribution  $\sigma_{xy}$  for the R-C series beam,  $t = 100$  days

Based on the above results, the effect of prestressing on the RS series beam is more pronounced than on the R-C series beam. Hence in the case of the R-C series beam, tensile stresses are formed in the lower layer when loaded with a given  $F_{sust}$  force.  $\sigma_{xx} = 18.8$  MPa, while in the R-S series beam, compressive stresses of the order of 100 MPa are observed in the area under the same load.

The stress distribution pattern  $\sigma_{xy}$  is of particular interest for the investigated beam schemes (Fig. 23 and 25). Comparing the data in Fig. 23 and 25, we find that the voltage field is more uniform.  $\sigma_{xy}$  corresponds to the R-S series beam. Minor disturbances in the distribution  $\sigma_{xy}$  for this beam, it is observed at the place of application of the load and the area adjacent to the support. It should be noted that the background reinforcement for the beams of both series was assigned to be almost identical.

**Discussion and Conclusion.** The analysis of the distribution of displacements and stresses in the considered reinforced concrete beams considering the creep of concrete and the pre-stress generated by the cable reinforcement thus enables the following conclusions to be made.

1. The distributed scheme of "background" reinforcement from a physical point of view allows the most realistic modelling of the joint work of the reinforcing frame and the concrete array.

2. The suggested concept for identifying the restoring force caused by the tension of the "active" reinforcement can be implemented in the software complexes ANSYS, Lira CAD and SCAD Office certified by the Russian Academy of Architecture and Building Sciences.

3. It was found that the deflection values of the beams obtained numerically and experimentally for time points 28 days and 100 days almost coincide.

4. The analysis of the longitudinal and tangential stress fields in the beams of the R-C and R-S series for a time of 100 days revealed a considerable effect of the "active" reinforcement scheme on the load-bearing capacity of the structures in terms of the appearance of tensile stresses in concrete. The developed mathematical and software allows the accuracy and reliability of strength calculations of monolithic prestressed girder structures made of reinforced concrete to be improved.

## References

1. Harutyunyan NH. *Some Issues of the Theory of Creep*. Moscow: Gostekhteorizdat; 1952. 323 p. (In Russ.).
2. Harutyunyan NH, Zevin AA. *Calculation of Building Structures Considering Creep*. Moscow: Stroyizdat; 1988. 256 p. (In Russ.).
3. Aleksandrovsky SV. *Calculation of Concrete and Reinforced Concrete Structures for Temperature and Humidity Changes Considering Creep*. Moscow: Stroyizdat; 1973. 432 p. (In Russ.).
4. Prokopovich IE, Zedgenidze VA. *Applied Theory of Creep*. Moscow: Stroyizdat; 1980. 240 p. (In Russ.).
5. Kharlab VD. *Fundamental Issues of the Linear Theory of Creep (in Relation to Concrete)*. St. Petersburg: SPbGASU; 2014. 207 p. (In Russ.).
6. Dikonov VP. *The MAPLE Mathematical System in R3/R4/R5*. Moscow: SOLON; 1998. 399 p. (In Russ.).
7. Gaydzhurov PP, Iskhakova ER. *Models of Concrete Creep Theory and their Finite Element Implementation*. Bulletin of DSTU. 2012;7:99-107. (In Russ.) URL: <https://www.vestnik-donstu.ru/jour/article/view/654/653> (accessed: 05.01.2025)
8. Ross AD. Creep of Concrete under Variable Stress. *Journal of the American concrete institute*. 1958;54(3):739–758. <https://doi.org/10.14359/11466>
9. Gaydzhurov PP, Iskhakova ER. *Finite Element Solution of the Planar Issue of the Theory of Hereditary Aging of Concrete Considering the Principle of Superposition of Impacts and Fast-Moving Creep of the Material (Polygon)*. Certificate of State Registration of the Computer Program No. 201462079. 2014. (In Russ.).
10. Gaydzhurov PP, Iskhakova ER, Savelyeva NA. Numerical Modeling of the Volumetric Stress-Strain of Prestressed Reinforced Concrete Structures Considering the Creep of Concrete. News of higher educational institutions. *The North Caucasus region*. Technical Sciences. 2023;2:17-24. (In Russ.) <http://dx.doi.org/10.17213/1560-3644-2023-2-17-24>
11. Reybrouck N, Van Mullem T, Taerwe L, Caspeele R. Influence of long-term creep on prestressed concrete beams in relation to deformations and structural resistance: Experiments and modeling. *Structural Concrete*. 2020;21(4):1458–1474. <https://doi.org/10.1002/suco.201900418>

## About the Authors:

**Peter P. Gaydzhurov**, Dr.Sci. (Eng.), Professor of the Department of Structural Mechanics and Theory of Structures, Don State Technical University (1 Gagarin Square, Rostov-on-Don, 344003, Russian Federation), [ORCID](#), [gpp-161@yandex.ru](mailto:gpp-161@yandex.ru)

**Elvira R. Iskhakova**, Cand.Sci. (Eng.), Associate Professor of the Department of Urban Planning, Design of Buildings and Structures, Platov South Russian State Polytechnic University (NPI) (132 Prosveshcheniya St., Novocherkassk, 346428, Russian Federation), [ORCID](#), [elvira.ishakova@yandex.ru](mailto:elvira.ishakova@yandex.ru)

**Nina A. Savelyeva**, Cand.Sci. (Eng.), Senior Lecturer of the Department of Structural Mechanics and Theory of Structures, Don State Technical University (1 Gagarin Square, Rostov-on-Don, 1344003, Russian Federation), [ORCID](#), [ninasav86@mail.ru](mailto:ninasav86@mail.ru)

## Claimed contributorship:

**PP Gaydzhurov**: basic concept formulation, selecting the solution method, analysis and generalization of the research results.

**ER Iskhakova**: writing and fixing the software code, preparing the original data for numerical modelling.

**NA Savelyeva**: developing the mathematical model of concrete creep, working with the text of the manuscript, analysis and generalization of the research results.

**Conflict of interest statement: the authors do not have any conflict of interest.**

**All authors have read and approved the final version of manuscript.**

## Об авторах:

**Гайджуров Петр Павлович**, доктор технических наук, профессор кафедры строительной механики и теории сооружений Донского государственного технического университета (344003, Российская Федерация, г. Ростов-на-Дону, пл. Гагарина, 1), [ORCID](#), [gpp-161@yandex.ru](mailto:gpp-161@yandex.ru)

**Исхакова Эльвира Рашидовна**, кандидат технических наук, ассистент кафедры градостроительства, проектирования зданий и сооружений Южно-Российского государственного политехнического университета им. М.И.Платова (НПИ) (346428, Российская Федерация, г. Новочеркасск, ул. Просвещения, 132), [ORCID](#), [elvira.ishakova@yandex.ru](mailto:elvira.ishakova@yandex.ru)

**Савельева Нина Александровна**, кандидат технических наук, старший преподаватель кафедры строительной механики и теории сооружений Донского государственного технического университета (344003, Российская Федерация, г. Ростов-на-Дону, пл. Гагарина, 1), [ORCID, ninasav86@mail.ru](mailto:ninasav86@mail.ru)

***Заявленный вклад авторов:***

**П.П. Гайджуров:** постановка задачи, выбор метода решения, обсуждение результатов.

**Э.Р. Исхакова:** написание кода и отладка программного обеспечения, подготовка исходных данных для численного моделирования.

**Н.А. Савельева:** разработка математической модели ползучести бетона, подготовка текста, формулирование выводов.

***Конфликт интересов:*** авторы заявляют об отсутствии конфликта интересов.

***Все авторы прочитали и одобрили окончательный вариант рукописи.***

**Received / Поступила в редакцию** 14.01.2025

**Reviewed / Поступила после рецензирования** 30.01.2025

**Accepted Принята к публикации** 08.02.2025